Electronic Supplementary Information (ESI)

Pillar[5]arene Pseudo[1]rotaxanes-Based Redox-Responsive Supramolecular Vesicles for Controlled Drug Release

Ya-Han Cui,[a] Rong Deng,[a] Zheng Li,[a] Xu-Sheng Du,[a] Qiong Jia,[a] Xing-Huo Wang,[a] Chun-Yu Wang,[c] Kamel Meguellati,*[a] and Ying-Wei Yang*[ab]

[a]International Joint Research Laboratory of Nano-Micro Architecture Chemistry (NMAC), College of Chemistry, Jilin University, 2699 Qianjin Street, Changchun 130012, China

[b]The State Key Laboratory of Refractories and Metallurgy, School of Chemistry & Chemical Engineering, Wuhan University of Science and Technology, Wuhan 430081, China

[c]State Key Laboratory of Supramolecular Structure and Materials, Institute of Theoretical Chemistry, Jilin University, 2699 Qianjin Street, Changchun 130012, China

Corresponding Authors

*E-mail: kamel_m@jlu.edu.cn (K.M.); ywyang@jlu.edu.cn (Y.-W.Y.)

Contents

1. Materials and methods

4-Methoxyphenol, ethyl bromoacetate, 1, 4-dimethoxybenzene, borontrifluoride diethyl etherate, paraformaldehyde and cystamine dihydrochloride were purchased from Aladin and used as received. All other reagents were commercially available and used as supplied without further purification. Solvents were employed as purchased.

NMR spectra were recorded on a Mercury-300BB-300 MHz spectrometer and a Bruker 400 MHz spectrometer using the deuterated solvent as the lock and the residual solvent or TMS as the internal reference. Data are presented as follows: chemical shift, multiplicity (s=singlet, d=doublet, t=triplet, q=quartet, m=multiplet), coupling constants in Hertz (Hz), integration. Low-resolution electrospray ionization (LR-ESI) mass spectra were obtained on a Bruker Esquire 3000 plus mass spectrometer (Bruker-Franzen Analytik GmbH Bremen, Germany) equipped with an ESI interface and an ion trap analyzer. High-resolution electrospray ionization (HRESI) mass spectra were obtained on a Bruker 7-Tesla FT-ICR mass spectrometer equipped with an electrospray source (Billerica, MA, USA). Fourier transform infrared (FT-IR) spectra were collected on a Vertex 80 V spectrometer. Thin-layered chromatography (TLC) was performed using silica gel 60 F254 plates. Scanning electron microscope (SEM) images were recorded on a HITACHI SU8082 instrument. Transmission electron microscope (TEM) images were performed on a Tecnai G2 S-Twin F20 instrument. Dynamic light scattering (DLS) measurements were performed on a Zetasizer Nano ZS instrument. The controlled release experiments were recorded via UV-vis spectroscopy on a Shimadzu UV-1800 spectrophotometer.

2. Experimental section

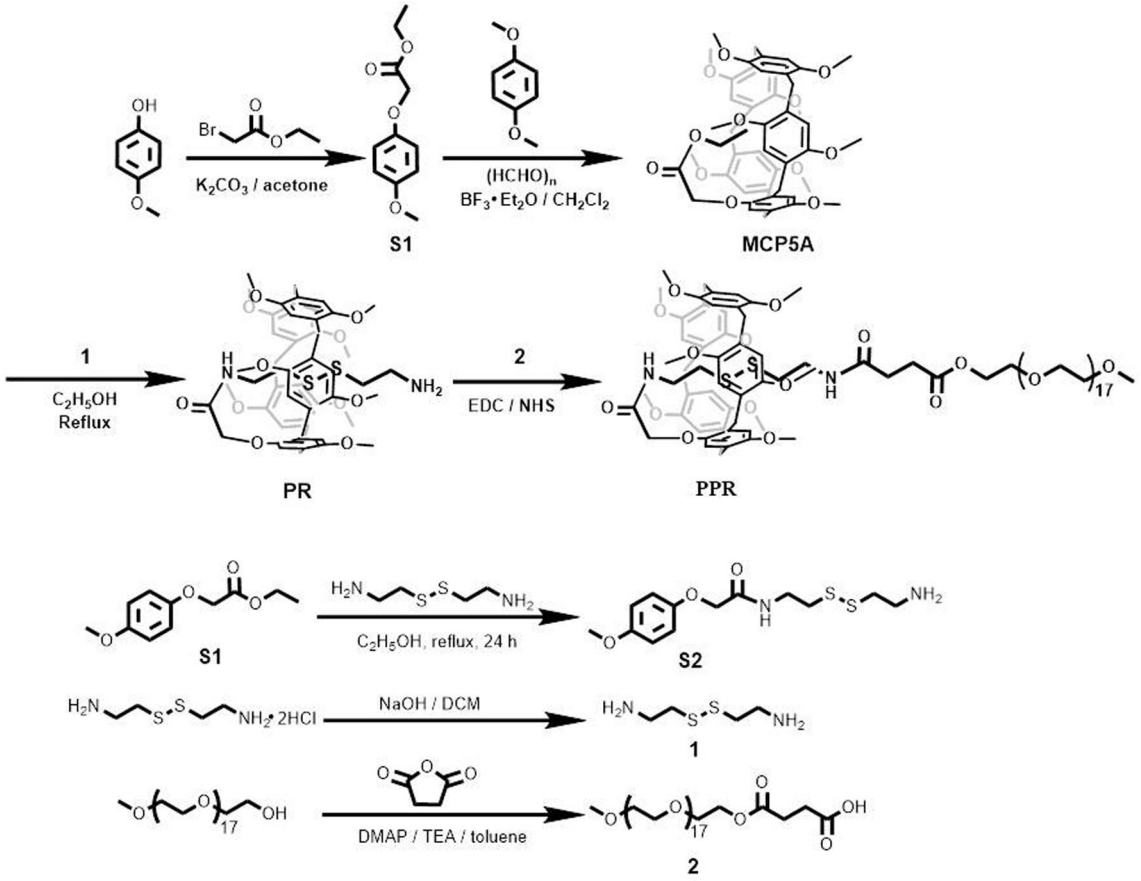

Scheme S1. Synthetic route to the amine-terminated pillar[5]arene-based pseudo[1]rotaxane (**PR**) and the amphiphilic pillar[5]arene-based pseudo[1]rotaxane (**PPR**).

Compound **S1** and **MCP5A** were prepared based on our previously reported procedures.[S1] Compounds **1** and **2** were also easily synthesized according to literature procedures.

Synthesis of compound PR. Cystamine dihydrochloride was neutralized by 4 M sodium hydroxide (NaOH) and extracted with dichloromethane (CH_2Cl_2) to yield cystamine (**1**).[S2, S3] **MCP5A** (200 mg, 0.24 mmol) was dissolved in ethanol (3 mL) under stirring at 80 ℃ in a 10 mL round-bottom flask. Then a solution of cystamine (370 mg, 2.4 mmol) was added into the flask and stirred for another 60 h. After completion of reaction, the solvent was evaporated under reduced pressure. The crude product was purified by column chromatography on silica

gel (CH_2Cl_2:MeOH=10:1) to give the compound **PR** as a yellowish solid (107 mg, 54%). ^{1}H NMR (400 MHz, $CDCl_3$, 298 K) δ (ppm): 7.02–6.60 (m, 10H), 6.66 (t, J = 5.0 Hz, 1H), 4.49 (s, 2H), 3.90–3.60 (m, 37H), 2.98 (s, 2H), 1.73–1.56 (m, 2H), 0.98 (t, J = 6.3 Hz, 2H), 0.79 (t, J = 6.3 Hz, 2H). ^{13}C NMR (101 MHz, $CDCl_3$, 298 K) δ (ppm): 169.34, 151.46, 151.08, 150.95, 150.91, 150.86, 150.79, 150.58, 150.52, 150.50, 149.39, 129.38, 129.31, 129.05, 128.97, 128.91, 128.76, 128.57, 128.32, 128.24, 127.23, 114.94, 114.50, 114.42, 114.13, 113.98, 113.94, 113.51, 69.17, 56.60, 56.30, 56.21, 56.14, 56.11, 55.94, 55.89, 55.66, 42.44, 40.07, 39.76, 36.35, 30.57, 29.67, 29.44, 28.87, 28.79. HR-ESI-MS: m/z calcd. for $[M+H]^+$ $C_{50}H_{61}N_2O_{11}S_2^+$, 929.3711; found 929.3456.

Synthesis of compound PPR. PR (150 mg, 0.16 mmol) and mPEG-COOH (**2**) (M_n=750 g/mol, 600 mg, 0.80 mmol) were dissolved in anhydrous CH_2Cl_2 (10 mL). The mixture was added dropwise to a solution of N,N'-dicyclohexylcarbodiimide (DCC, 49 mg, 0.24 mmol) and 4-dimethylaminopyridine (DMAP, 5 mg, 0.04 mmol) at 0 ℃. The above solution was kept for another 24 h at room temperature. Then the white precipitate was filtered off and the filtrate was concentrated under vacuum. The residue was purified by silica gel column chromatography (CH_2Cl_2:MeOH=50:1) to produce **PPR** as a yellowish transparent liquid (100 mg, 35%). ^{1}H NMR (300 MHz, $CDCl_3$, 298 K) δ (ppm): 0.851 (m, 4H, -S*CH$_2$CH$_2$*NH-), 1.89 (m, 2H, -NHCH$_2$*CH$_2$*S-), 2.63 (m, 4H, -OOC*CH$_2$CH$_2$*COOH), 2.98 (m, 2H, -NH*CH$_2$*CH$_2$S-), 3.38 (s, 3H, *CH$_3$*O-), 3.71-3.46 (m, -O*CH$_2$CH$_2$*O-, -ArO*CH$_3$*), 3.76 (s, 10H, -Ar*CH$_2$*Ar-), 4.26 (m, 2H, -*CH$_2$*OOC-), 4.46 (s, 2H, -ArO*CH$_2$*CO-), 6.98-6.78 (m, 10H, Ar*H*).

Synthesis of N-(2-((2-aminoethyl)disulfaneyl)-2-(4-methoxyphenoxy) acetamide (S2). A mixture of ethyl-4-methoxy phenoxy acetate (**S1**, 200 mg, 0.95 mmol) and cystamine (289

mg, 1.90 mmol) in ethanol (5.0 mL) were stirred in a 10 mL round-bottom flask at reflux for 60 h. Furthermore, the residue was concentrated. The obtained mixture was purified by column chromatography on silica gel (CH_2Cl_2:MeOH=10:1) to give a yellowish powder (130 mg, 43.3%). ^{1}H NMR (300 MHz, $CDCl_3$, 298 K) δ (ppm): 7.04 (s, 1H), 6.86 (d, J = 2.1 Hz, 4H), 4.45 (s, 2H), 3.78 (s, 3H), 3.70 (q, J = 6.3 Hz, 2H), 3.02 (dd, J = 11.1, 5.1 Hz, 2H), 2.84 (t, J = 6.4 Hz, 2H), 2.77 (t, J = 6.1 Hz, 2H), 1.46 (s, 2H). ^{13}C NMR (75 MHz, $CDCl_3$, 298 K) δ (ppm): 168.95, 155.02, 151.60, 115.99, 115.12, 68.45, 55.97, 42.70, 40.81, 38.10, 37.85. LC-ESI-MS: m/z calcd for $[M+H]^+$ (100.00%) $C_{13}H_{21}N_2O_3S_2^+$, 317.0988; found 317.0950.

Synthesis of mPEG-COOH (2). mPEG-OH (M_n=750 g/mol, 1.5 g), succinic anhydride (300 mg, 3.0 mmol) and 4-dimethylaminopyridine (24 mg, 0.2 mmol) were dissolved in anhydrous toluene (5.0 mL). After stirring for 15 min, the mixture was added to trimethylamine (202 mg, 2 mmol) dropwise. The crude solution was stirred overnight at 25 ℃. When the reaction finished, the mixture was concentrated. Then the residue was dissolved in CH_2Cl_2. This white product was further re-crystallization in petroleum ether for three times. ^{1}H NMR (300 MHz, $CDCl_3$, 298 K) δ (ppm): 2.65 (m, 4H, -OOC*CH$_2$CH$_2$*COOH), 3.38 (s, 3H, *CH$_3$*O-), 3.71-3.54 (m, -O*CH$_2$CH$_2$*O-), 4.26 (t, 2H, -*CH$_2$*OOC-).

Fabrication of non-loaded PPR vesicles and DOX-loaded DPPR vesicles. The DOX-loaded vesicles were prepared via a nanoprecipitation method according to the literature.[S4, S5] Briefly, **PPR** (10 mg，0.01 mmol) and doxorubicin hydrochloride (DOX, 5 mg, 0.01 mmol) were dissolved in THF (3 mL) and stirred vigorously for 2 h. Then, the reaction mixture was added dropwise into deionized water (10 mL) to give an aqueous dispersion of amphiphilic complex. After stirring for 2 h, THF was removed by a dialysis method

(M_w=1000 Da) for two days. The obtained DOX-encapsulated nanoparticles were stored in 4 ℃ refrigerator before use. Empty **PPR** vesicles were also prepared via the same nanoprecipitation method mentioned above. The DOX loading capacity (LC) and encapsulation efficiency (EE) were calculated as:

$$\text{Drug loading capacities(LC)}=\frac{\text{weight of loaded DOX}}{\text{weight of total vesicle}}\times 100\%$$

$$\text{Drug encapsulation efficiencies(EE)}=\frac{\text{weight of loaded DOX}}{\text{weight of total added DOX}}\times 100\%$$

Determination on the CMC of PPR vesicles. The CMC was determined using fluorescence spectroscopy in the presence of pyrene, a hydrophobic probe. Briefly, a pyrene solution (1.2 mmol L^{-1}) were prepared in acetone,[S6] which was added into a series of 2 mL volumetric flasks in very small amounts. After the solvent was evaporated, the **PPR** solutions were added into deionized water to obtain the mixture with serial concentrations ranging from 0.1 to 2000 μg/mL and further sonicated for 1 h. The excitation (λ_{ex}) and emission (λ_{em}) wavelengths were 335 and 390 nm, respectively.

Redox-responsive experiments of DOX-loaded vesicles. A reduction condition, simulating the intracellular circumstance, was conducted to study the GSH-triggered conformation change of the vesicles. We exposed DOX-loaded nanoparticles to different concentrations of GSH to test the redox-sensitivity of the nanoaggregates. The release profile of DOX from vesicles was further performed by using a dialysis method. The abovementioned vesicular solution was moved into a dialysis tube (M_w=1000 Da). Then, it was immersed in deionized water with various amounts of GSH (0 mM, 5 mM and 10 mM) and gently stirred at room temperature. At predetermined time internals, the amount of released DOX was determined

using a UV-vis spectrophotometer at 475 nm.

Cytotoxicity assays. The cytotoxicity of DOX-unloaded **PPR** vesicles and DOX-loaded **DPPR** platform was evaluated by the CCK-8 assay using A549 cancer celline in 96-well cell culture plates.[S7] Briefly, the cells were cultured at 37 ℃ in 5% CO_2 in DMEM containing 10% FBS. Then, the cells were seeded at a density of 4000 cells/well and incubated for attachment. Then 2 μL of fresh culture medium containing different concentration of **PPR** solution, **DPPR** solution and free DOX were added into each well. Wells with media (without vesicles) were used as controls. The cells were further incubated for another 48 h and washed using PBS for twice. Cell viability was evaluated using CCK-8 cytotoxicity assay kit based on an established protocol and the optical densities were measured by spectraMax M_2 microplate reader at 450 nm. The experiments were conducted at least in triplicate.

Cellular uptake and intracellular localization. The cellular uptake and intracellular localization of free DOX and DOX-loaded **PPR** vesicles were examined by fluorescence microscope toward A549 cells. Briefly, cells were incubated in two chambered cover glasses for 48 h within the atmosphere of CO_2 at a temperature of 37 ℃. Then, we removed the culture medium, followed by the addition of DOX and **DPPR** (250 μg mL^{-1}) into each chamber. After incubation for another 4 h, 8 h and 12 h, the cells were washed with PBS for three times. The cytoskeleton was stained with Hoechst 33342 (10 μL) for another 10 min and washed three times with PBS. Then the cells were fixed with fresh 4.0% formaldehyde at 25 ℃ for 15 min. Images were acquired with confocal laser scanning microscopy.

3. Characterization of compounds

3.1. Characterization of S1

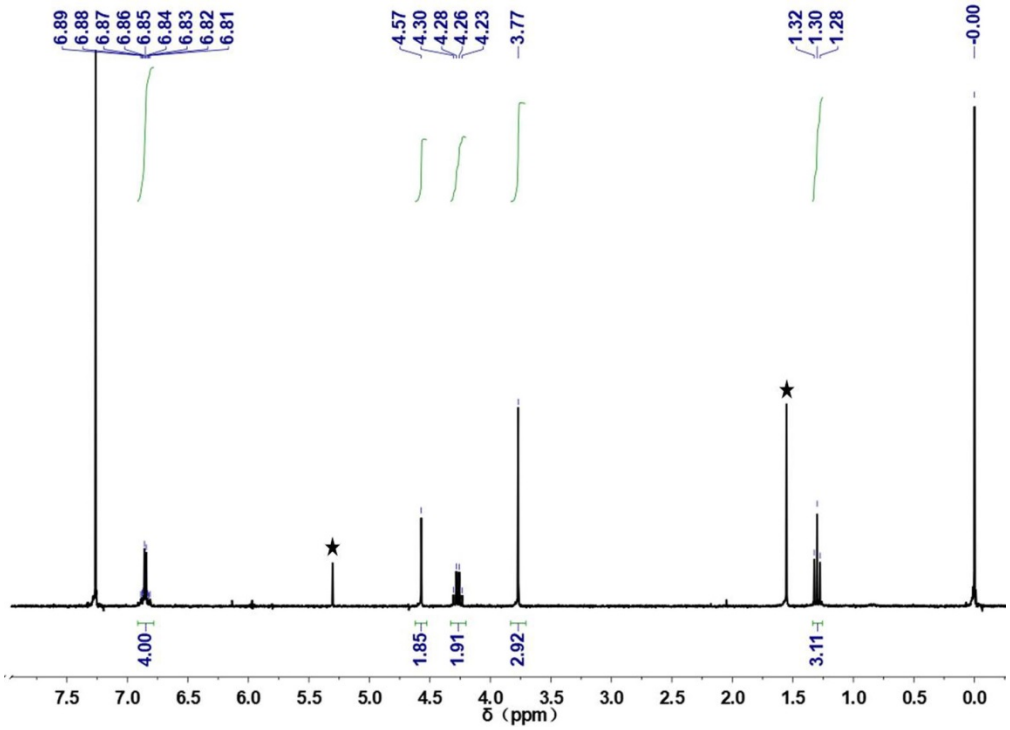

Figure S1. ^{1}H NMR spectrum (300 MHz, $CDCl_3$, 298 K) of **S1**.

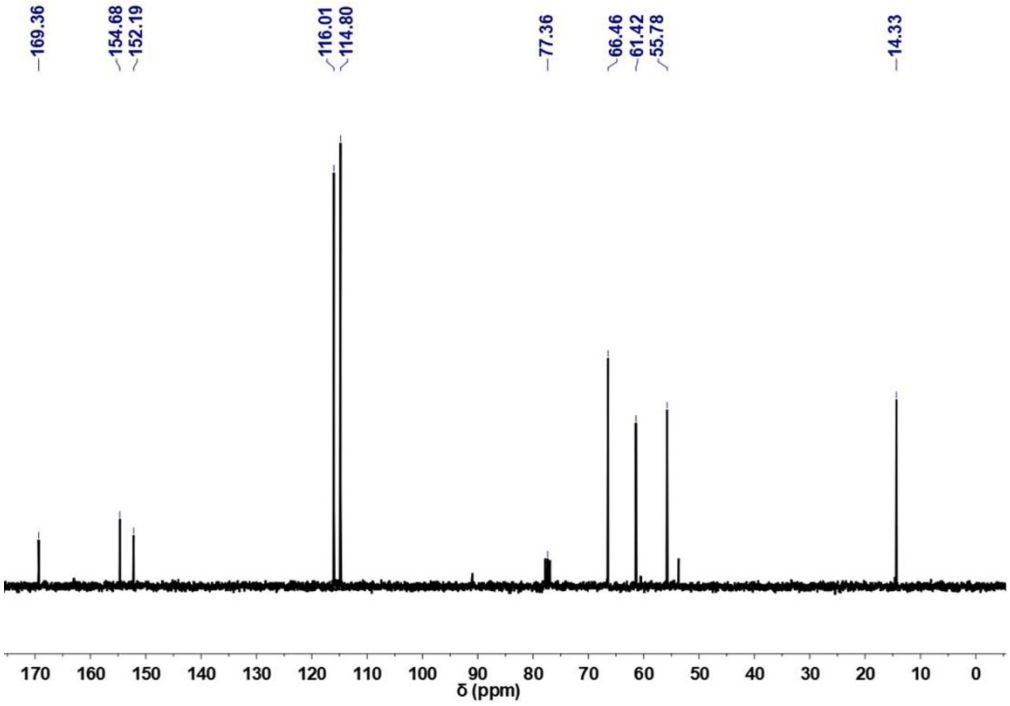

Figure S2. ^{13}C NMR spectrum (75 MHz, $CDCl_3$, 298 K) of **S1**.

3.2. Characterization of MCP5A

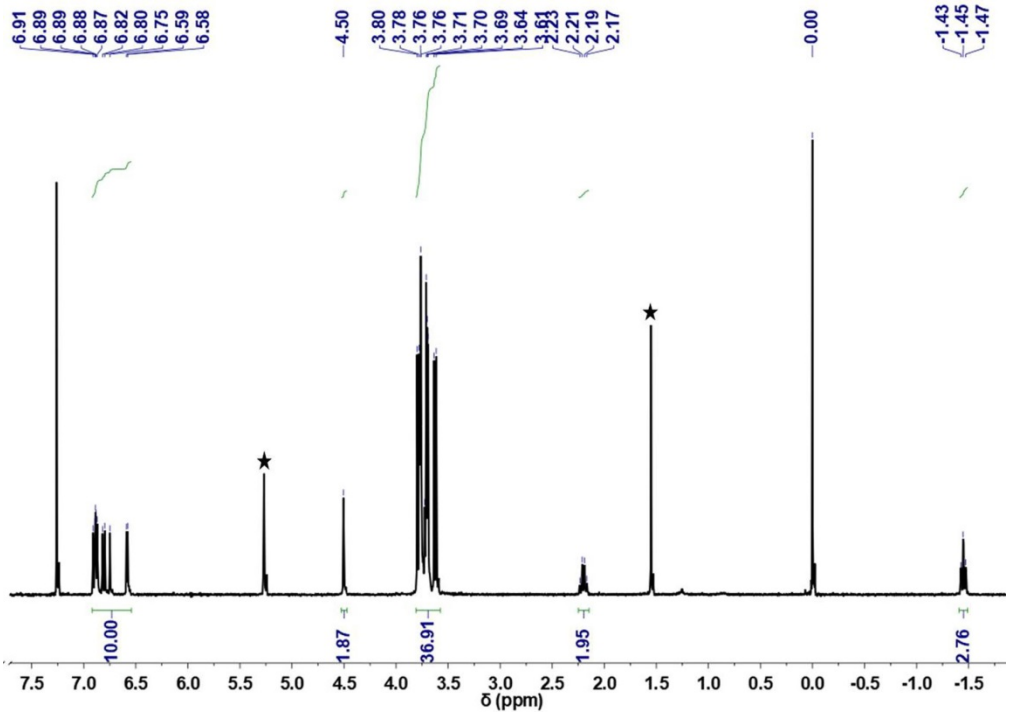

Figure S3. ^{1}H NMR spectrum (300 MHz, $CDCl_3$, 298 K) of **MCP5A**.

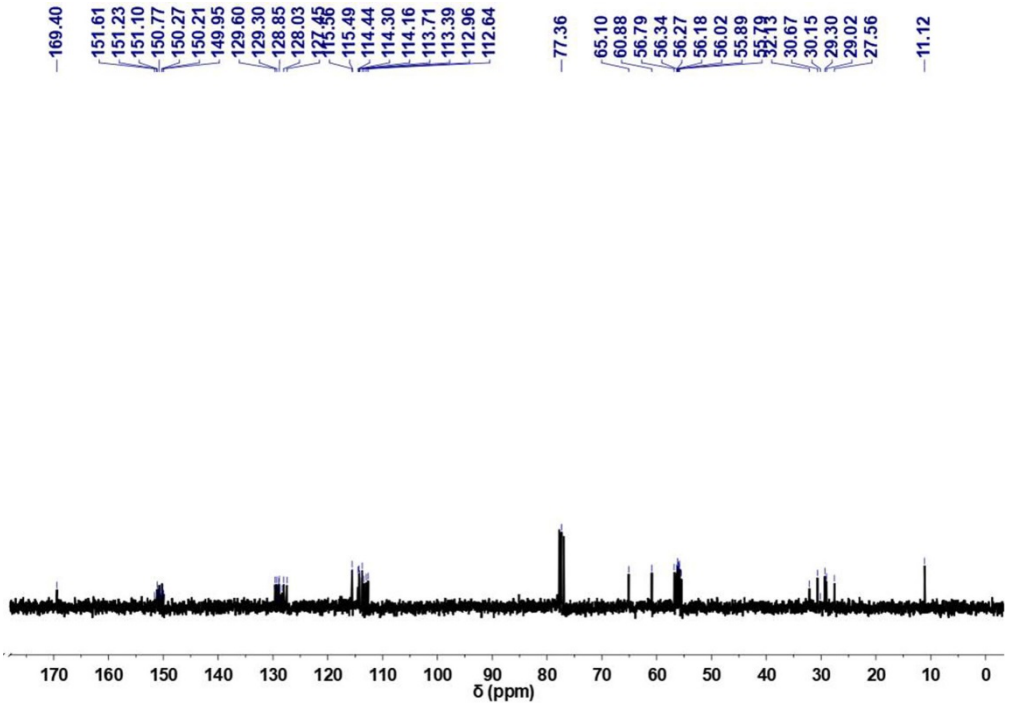

Figure S4. ^{13}C NMR spectrum (75MHz, $CDCl_3$, 298 K) of **MCP5A**.

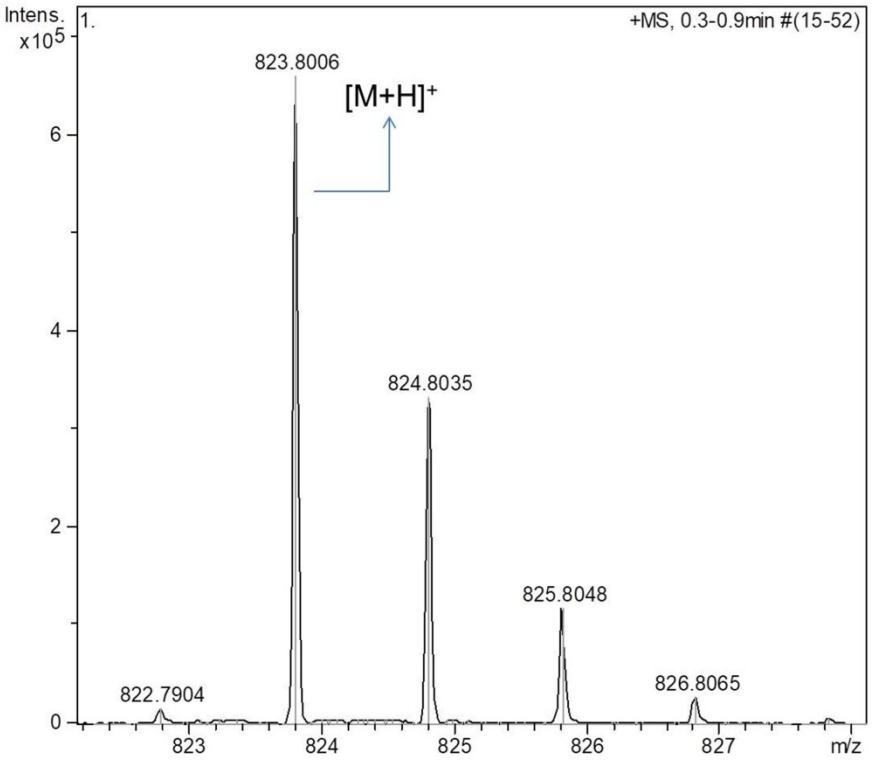

Figure S5. Mass spectrum of **MCP5A**. HR-ESI-MS: m/z calcd. for $[M+H]^+$ $C_{48}H_{55}O_{12}^+$, 823.3688; found 823.8006.

3.3. Characterization of PR

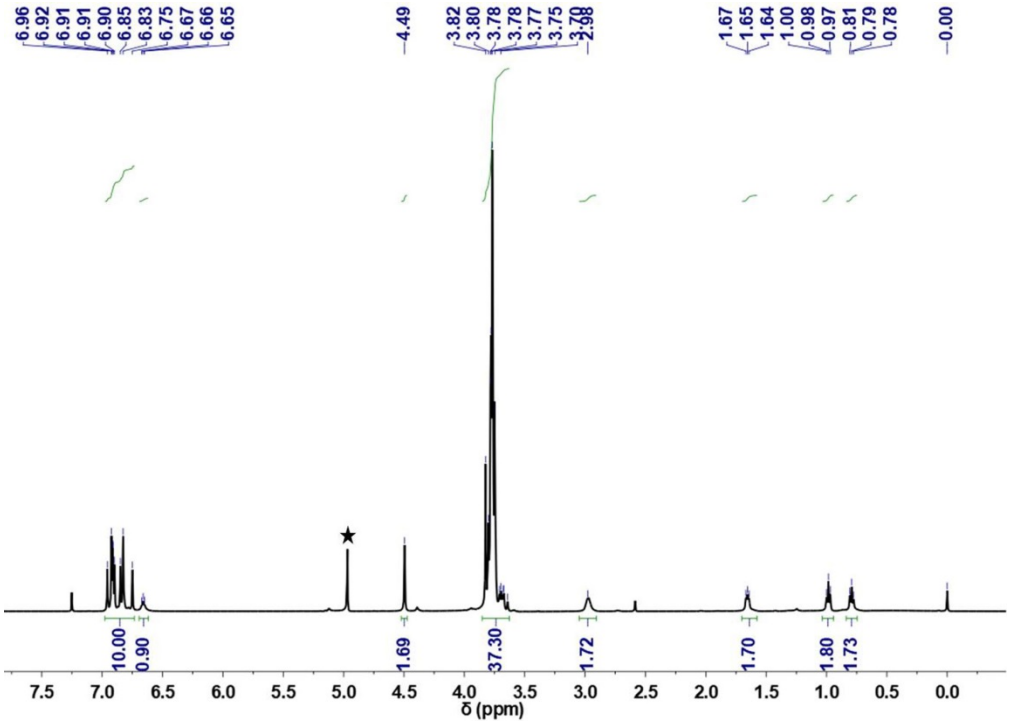

Figure S6. ^{1}H NMR spectrum (400 MHz, $CDCl_3$, 298 K) of **PR**.

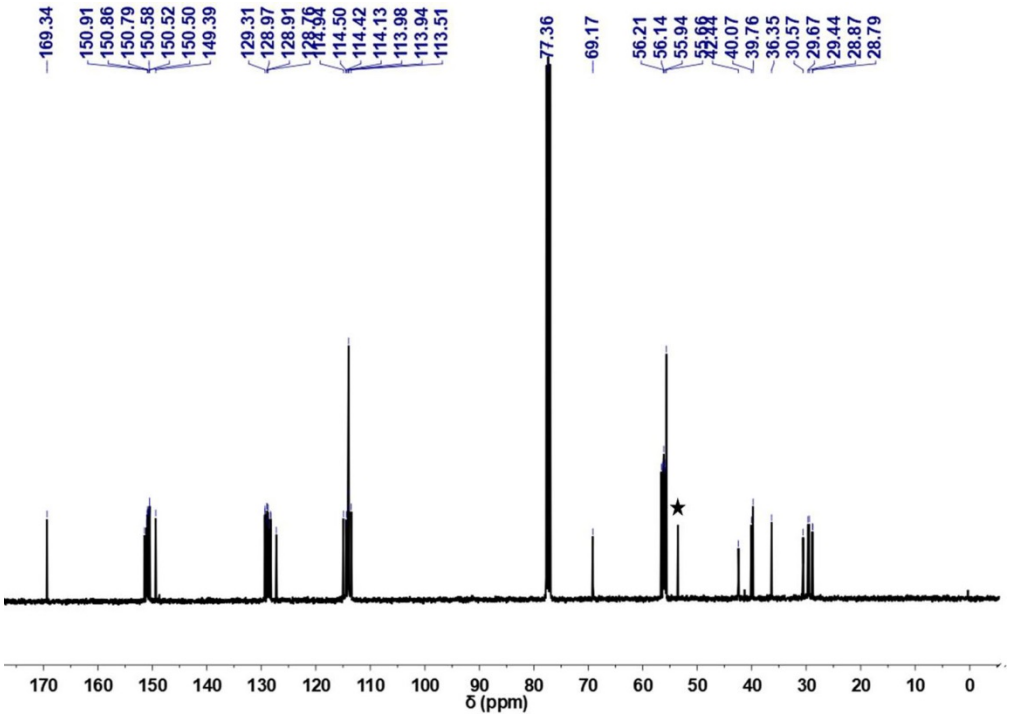

Figure S7. ^{13}C NMR spectrum (101MHz, $CDCl_3$, 298 K) of **PR**.

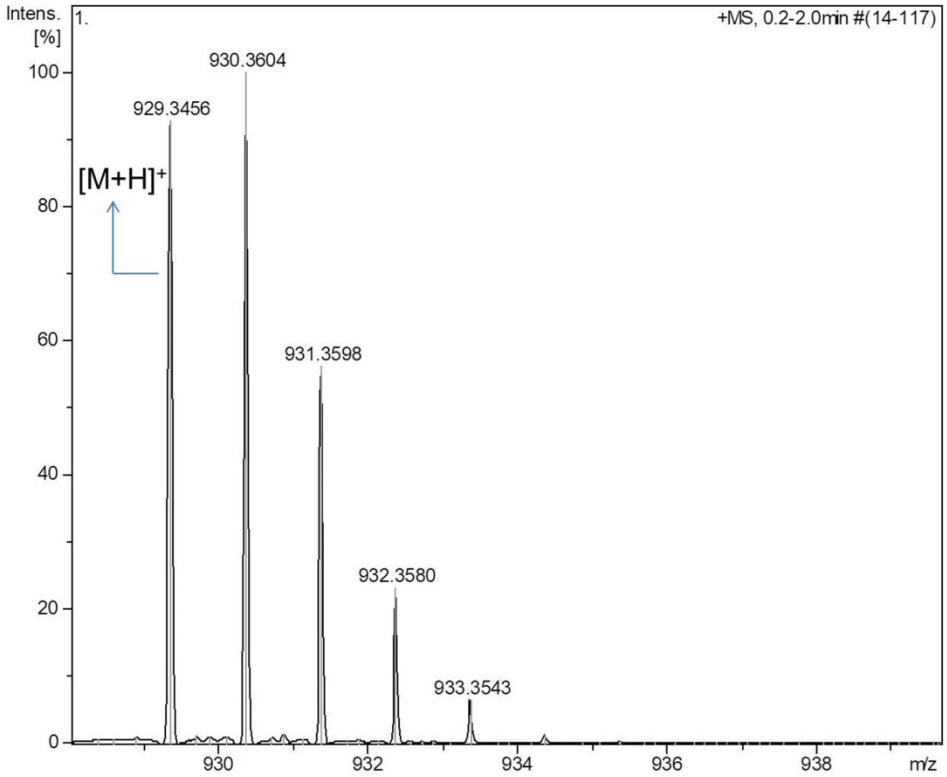

Figure S8. Mass spectrum of **PR**. HR-ESI-MS: m/z calcd. for $[M+H]^+$ $C_{50}H_{61}N_2O_{11}S_2^+$, 929.3711; found 929.3456.

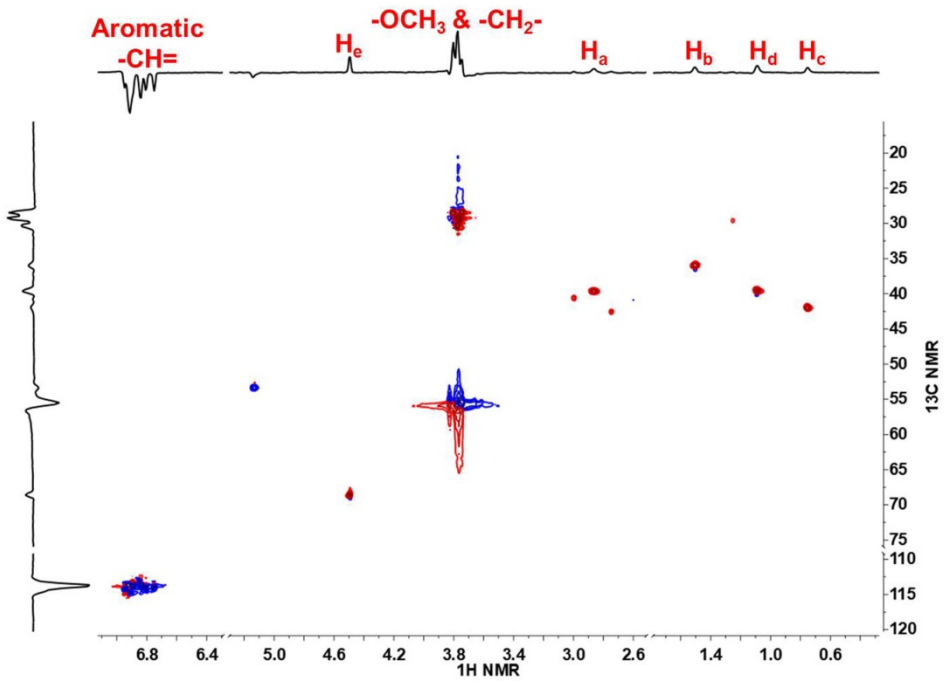

Figure S9. Full spectrum of HSQC to **PR**.

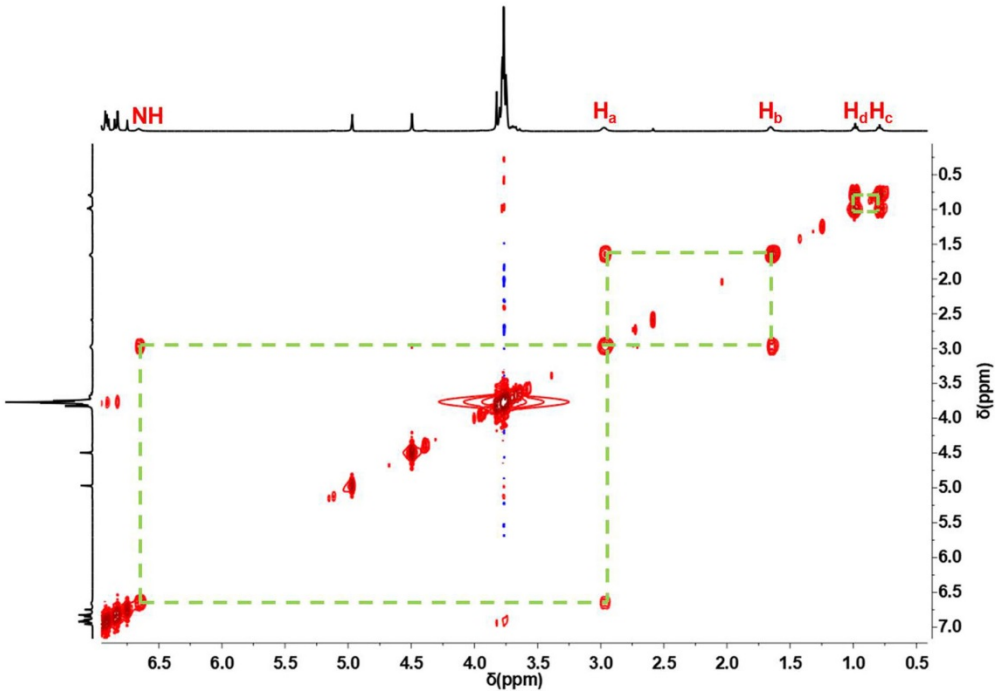

Figure S10. Partial spectrum of COSY to **PR**.

3.4. Characterization of PPR

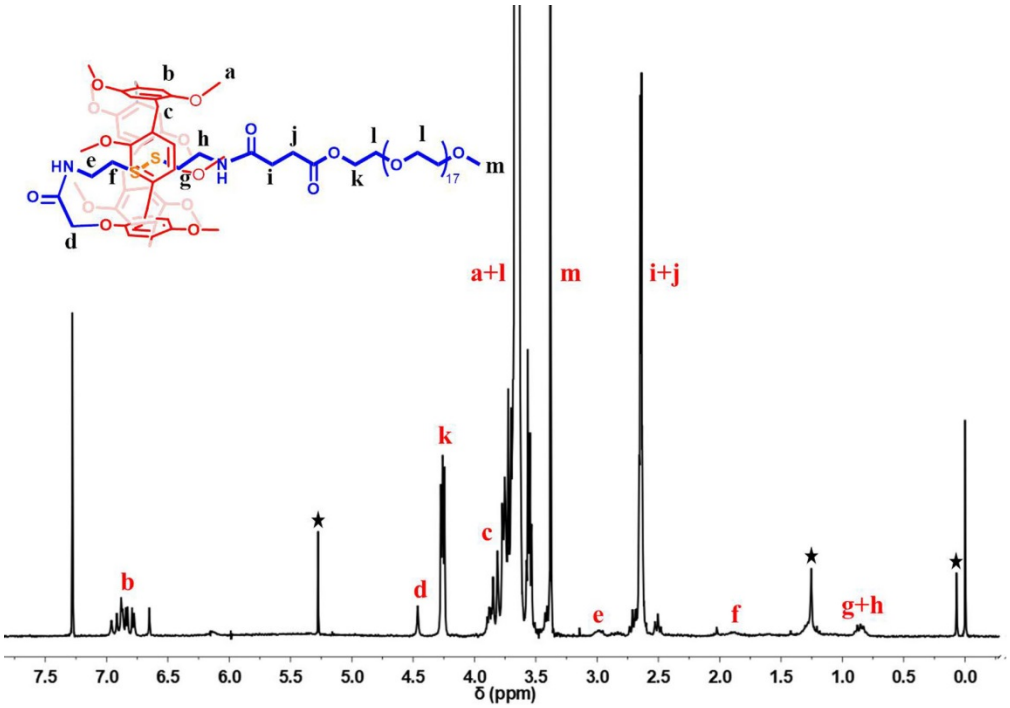

Figure S11. ^{1}H NMR spectrum (300 MHz, $CDCl_3$, 298 K) of **PPR**.

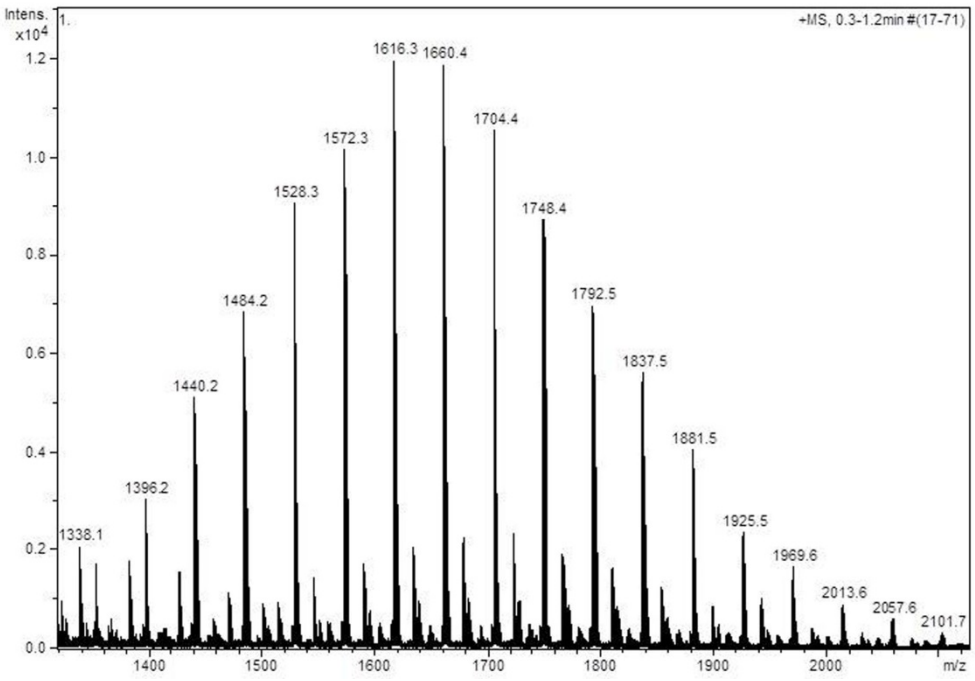

Figure S12. Mass spectrum of **PPR**.

3.5. Characterization of S2

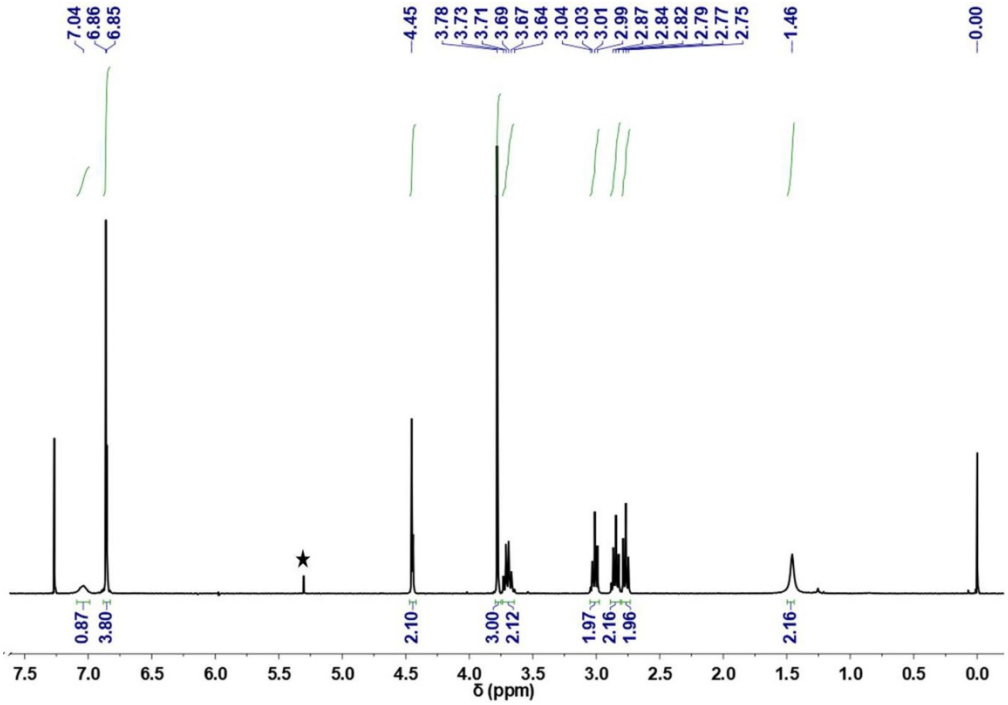

Figure S13. ^{1}H NMR spectrum (300 MHz, $CDCl_3$, 298 K) of **S2**.

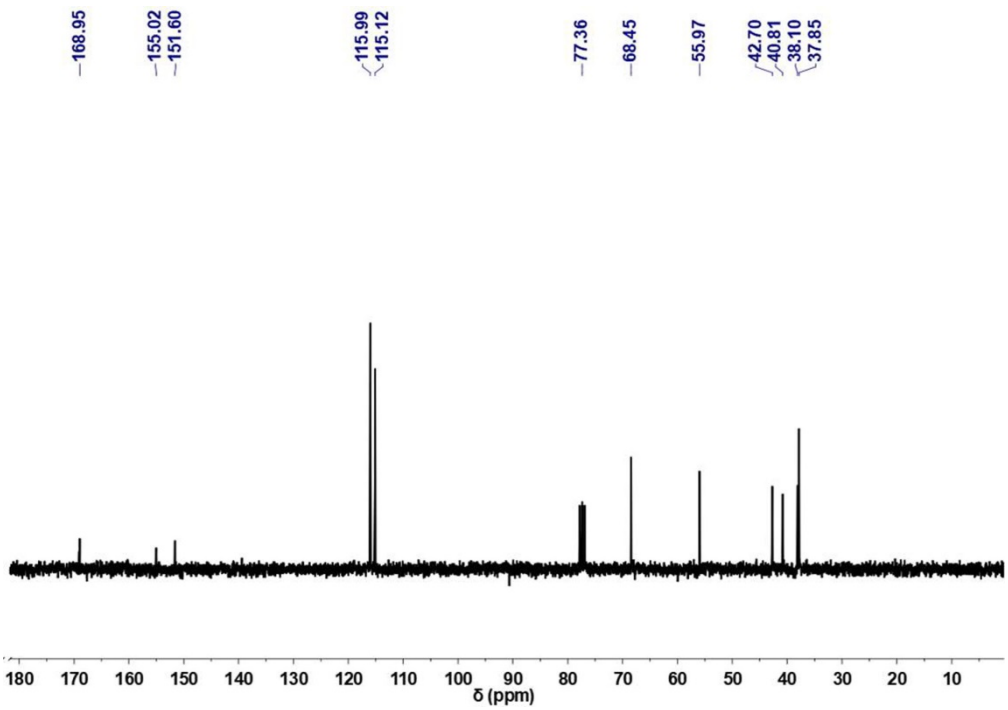

Figure S14. ^{13}C NMR spectrum (75 MHz, $CDCl_3$, 298 K) of **S2**.

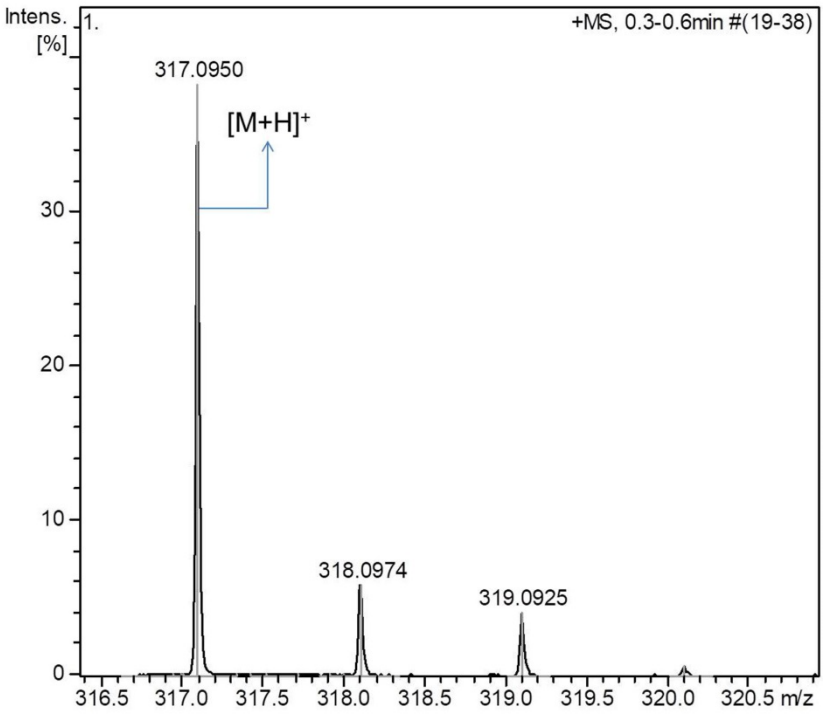

Figure S15. Mass spectrum of **S2**. HRESIMS: m/z calcd. for $[M+H]^+$ $C_{13}H_{21}N_2O_3S_2^+$, 317.0988; found 317.0950.

3.6. Characterization of 1

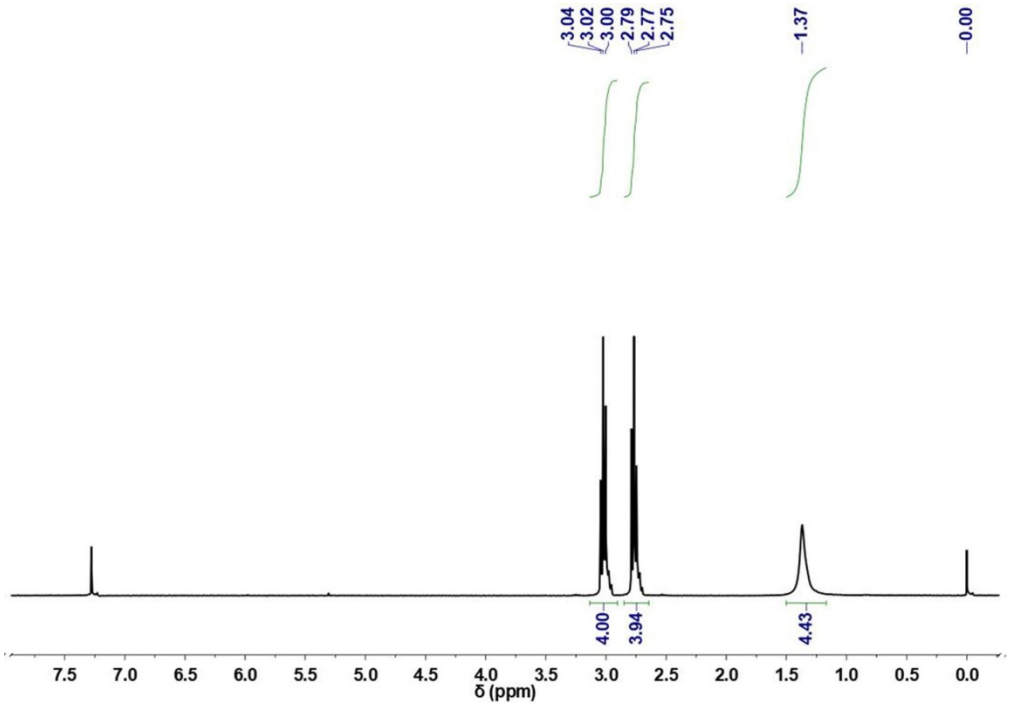

Figure S16. ^1H NMR spectrum (300 MHz, $CDCl_3$, 298 K) of **1**.

3.7. Characterization of 2

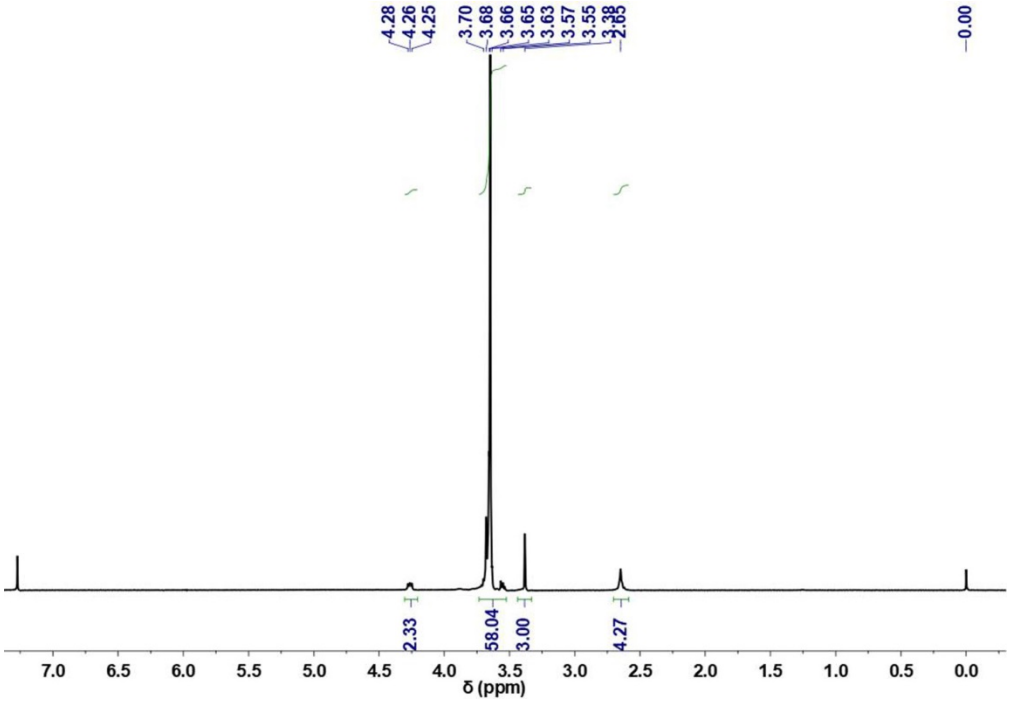

Figure S17. ^{1}H NMR spectrum (300 MHz, $CDCl_3$, 298 K) of **2**.

4. Concentration independent experiments of PR

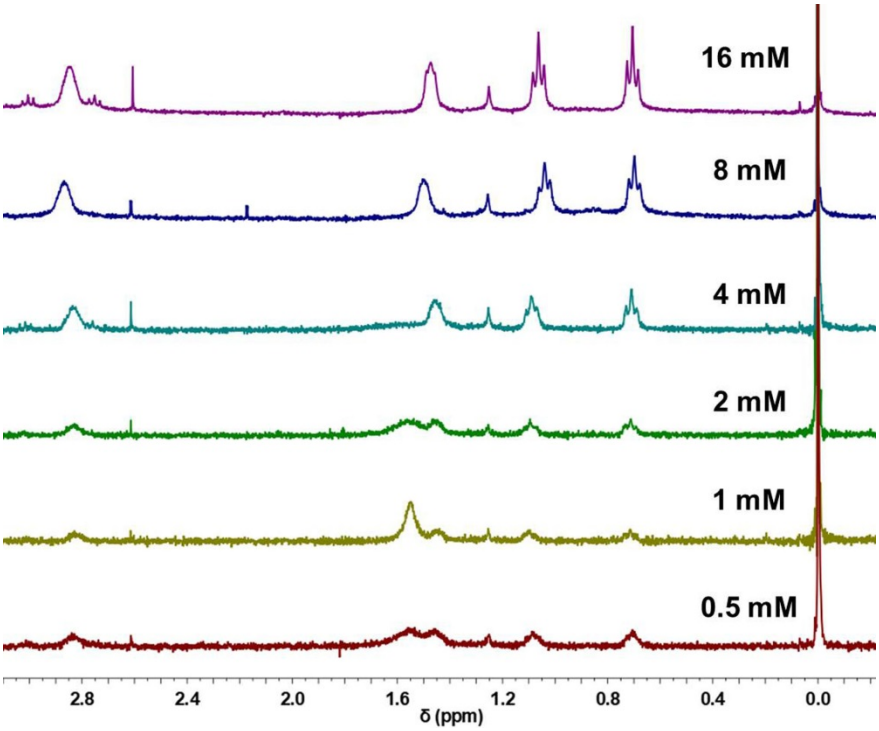

Figure S18. ^{1}H NMR spectra (300 MHz, $CDCl_3$, 298 K) of **PR** with variable concentration.

5. ^{1}H NMR spectroscopy of compound PPR in water

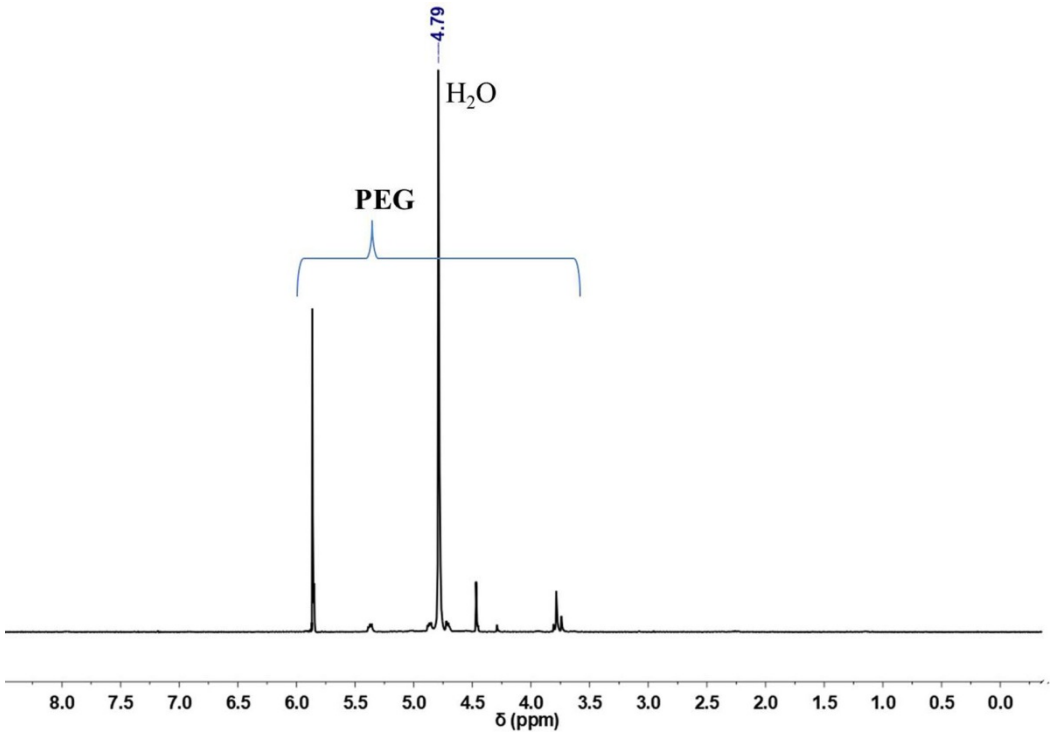

Figure S19. ^{1}H NMR spectrum (300 MHz, D_2O, 298 K) of **PPR**.

As shown in Figure S19, the ^{1}H NMR spectrum of **PPR** in D_2O only shows the proton resonances of PEG segment, which means that the pillar[5]arene part is shielded. According to the structure of **PPR**, the compound may form a vesicular-type structure. Furthermore, combined with the results of TEM and SEM experiments, we consider that it could form vesicles in water.

6. FT-IR spectra of compound MCP5A, PR and PPR

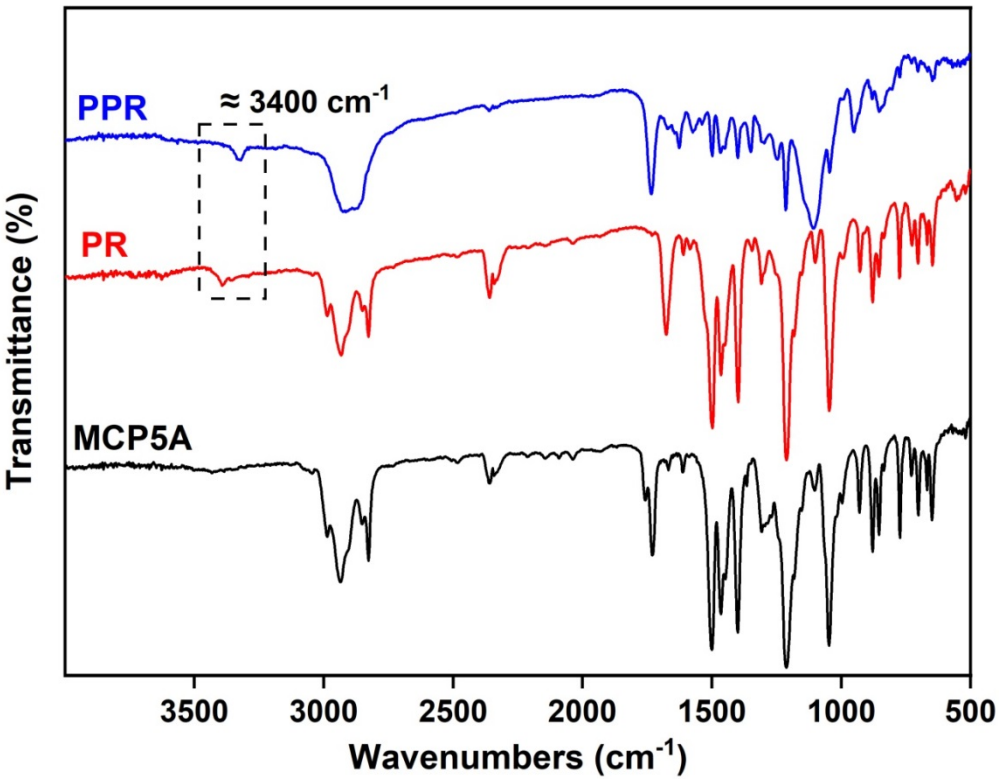

Figure S20. FT-IR spectra of **MCP5A**, **PR** and **PPR**.

7. ^{1}H NMR spectra of compound MCP5A, PR, PPR with malononitrile

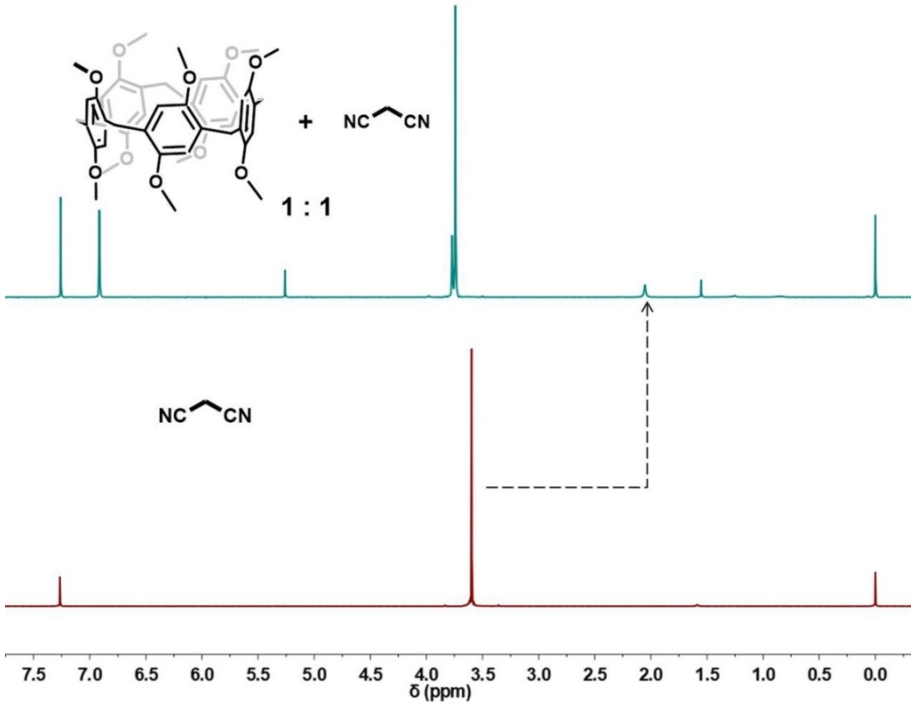

Figure S21. ^{1}H NMR spectra (300 MHz, $CDCl_3$, 298 K) of malononitrile and the competition systems after the addition of equal equivalent of **MCP5A**.

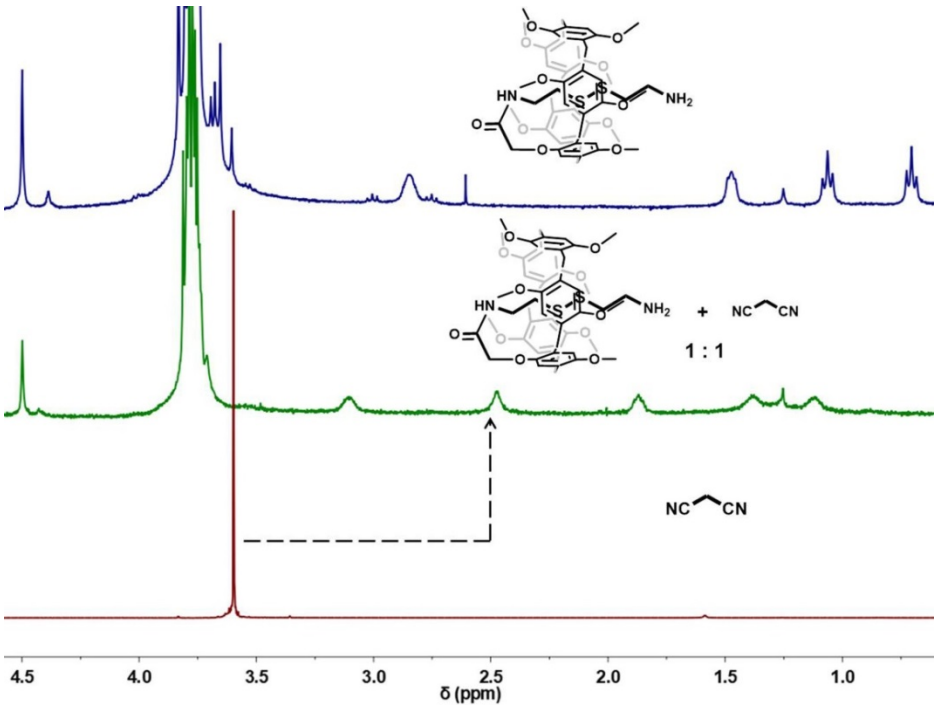

Figure S22. Partial ^{1}H NMR spectra (300 MHz, $CDCl_3$, 298 K) of **PR**, malononitrile and the mixed systems of **PR** after the addition of equal equivalent of malononitrile.

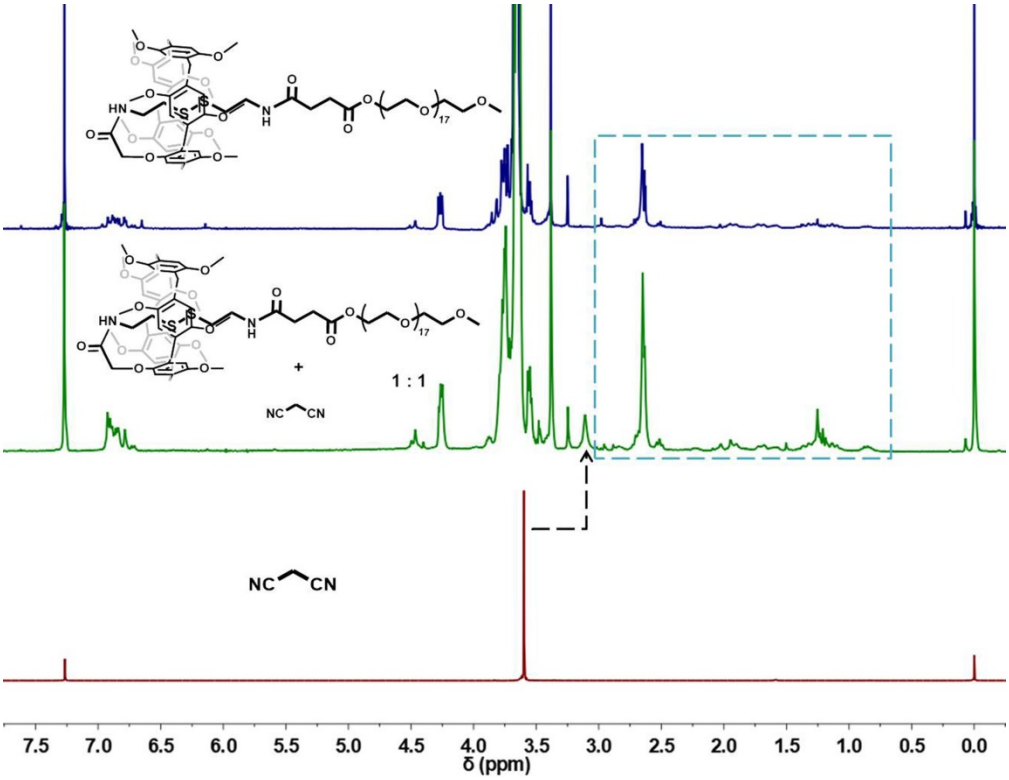

Figure S23. ^{1}H NMR spectra (300 MHz, $CDCl_3$, 298 K) of **PPR**, malononitrile and the mixed system of **PPR** after addition of equal equivalent of malononitrile.

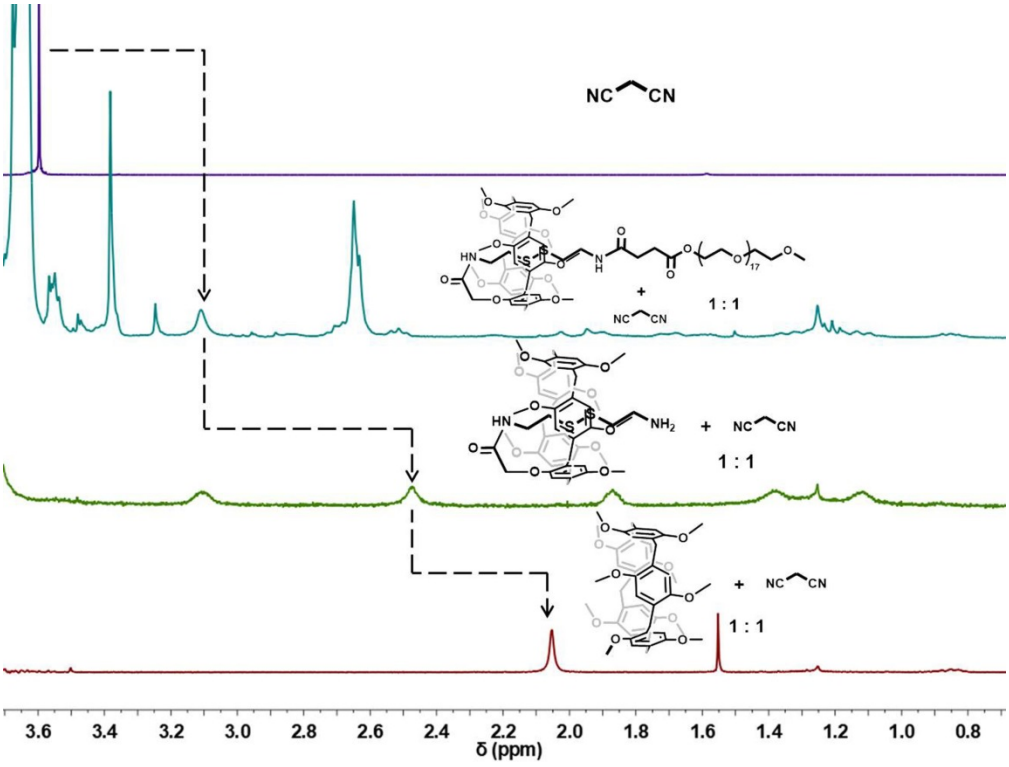

Figure S24. Partial ^{1}H NMR spectra (300 MHz, $CDCl_3$, 298 K) of **PPR**, **PR**, **MCP5A** with the additional of equal equivalent of malononitrile.

As shown in the above images, the ^{1}H NMR spectrum of malononitrile after the addition of equal equivalent of **PPR** upfield shifted slightly, whereas the proton resonances of **PPR** segment indicated the similar chemical shifts. To further investigate the reason for this phenomenon, corresponding ^{1}H NMR spectra of malononitrile with the addition of equal **MCP5A** and **PR**, respectively, are identified. By comparison, we can easily found that the characteristic peaks of malononitrile upfield shifted at different levels. It should be noted that there are strong binding ability of malononitrile with pillar[5]arene. The fact that the peaks of malononitrile upfield shifted significantly unambiguously indicates the inclusion of malononitrile in the cavity of pillar[5]arene. On the basis of the results obtained by ^{1}H NMR spectrum of after the addition of equal equivalent of **PPR**, we envisioned the slight change in the proton signals of malononitrile was attributed to flexible PEG segment of **PPR**, whereas **PPR** still kept the formation of self-inclusion complex, which again supports the excellent stability of self-inclusion formation of **PPR**.

8. UV-Vis spectra of DOX standard solution

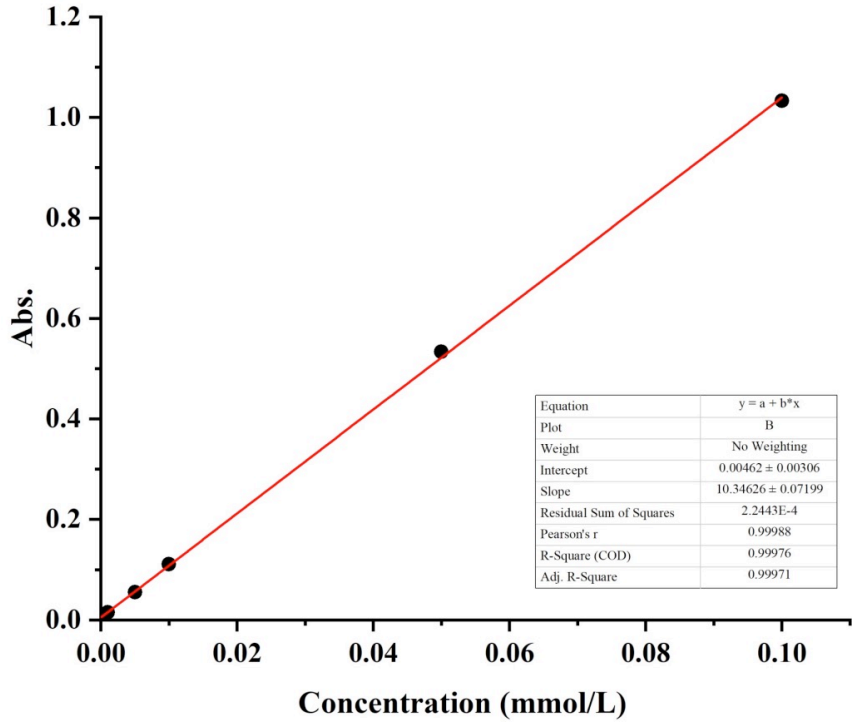

Figure S25. UV-Vis absorption spectra of DOX standard solution.

The standard curve equation of DOX solution: A=10.35•c+0.0046, R^2=0.9997.

9. Particle size measurement of DPPR with DOX loaded

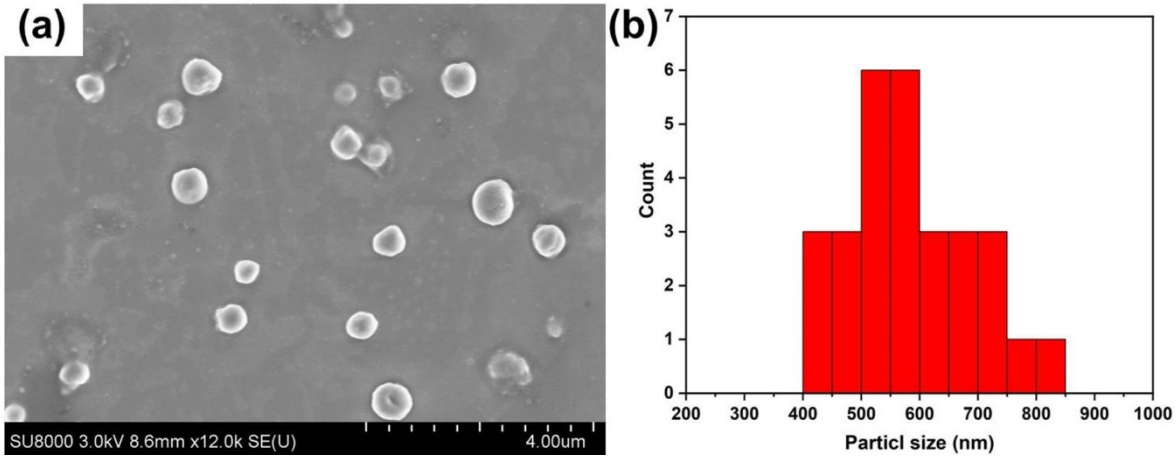

Figure S26. (a) SEM image of **DPPR** with DOX loaded. (b) The corresponding histogram of the size distribution of **DPPR**. The average diameter is ca. 550 nm.

10. References

S1. X. S. Du, C.-Y. Wang, Q. Jia, R. Deng, H.-S. Tian, H.-Y. Zhang, K. Meguellati and Y.-W. Yang, *Chem. Commun.,* 2017, **53**, 5326−5329.

S2. J. Wu, L. Zhao, X. Xu, N. Bertrand, W. Choi, B. Yameen, J. Shi, V. Shah, M. Mulvale, J. L. MacLean and O. C. Farokhzad, *Angew. Chem., Int. Ed.,* 2015, **54**, 9218−9223.

S3. R. Cheng, F. Meng, C. Deng, H.-A. Klok and Z. Zhong, *Biomaterials,* 2013, **34**, 3647−3657.

S4. R. Cheng, F. Feng, F. Meng, C. Deng, J. Feijen and Z. Zhong, *J. Controlled Release,* 2011, **152**, 2−12.

S5. X. Liu, K. Jia, Y. Wang, W. Shao, C. Yao, L. Peng, D. Zhang, X.-Y. Hu and L. Wang, *ACS Appl. Mater. Interfaces,* 2017, **9**, 4843−4850.

S6. M. Wilhelm, C. L. Zhao, Y. Wang, R. Xu, M. A. Winnik, J. L. Mura, G. Riess and M. D. Croucher, *Macromolecules,* 1991, **24**, 1033−1040.

S7. S. P. Hadipour Moghaddam, M. Yazdimamaghani and H. Ghandehari, *J. Controlled Release,* 2018, **282**, 62−75.